ANNALS OF LABORATORY MEDICINE

Comparison of Optical Genome Mapping With Conventional Diagnostic Methods for Structural Variant Detection in Hematologic Malignancies

Yeeun Shim ⓘ, M.S.[1,2],*, Yu-Kyung Koo ⓘ, M.D.[3],*, Saeam Shin ⓘ, M.D., Ph.D.[3], Seung-Tae Lee ⓘ, M.D., Ph.D.[3,4], Kyung-A Lee ⓘ, M.D., Ph.D.[3], and Jong Rak Choi ⓘ, M.D., Ph.D.[3,4]

[1]Brain Korea 21 PLUS Project for Medical Science, Yonsei University, Seoul, Korea; [2]MDxK (Molecular Diagnostics Korea), Inc., Gwacheon, Korea; [3]Department of Laboratory Medicine, Yonsei University College of Medicine, Seoul, Korea; [4]Dxome Co., Ltd., Seongnam, Korea

Background: Structural variants (SVs) are currently analyzed using a combination of conventional methods; however, this approach has limitations. Optical genome mapping (OGM), an emerging technology for detecting SVs using a single-molecule strategy, has the potential to replace conventional methods. We compared OGM with conventional diagnostic methods for detecting SVs in various hematologic malignancies.

Methods: Residual bone marrow aspirates from 27 patients with hematologic malignancies in whom SVs were observed using conventional methods (chromosomal banding analysis, FISH, an RNA fusion panel, and reverse transcription PCR) were analyzed using OGM. The concordance between the OGM and conventional method results was evaluated.

Results: OGM showed concordance in 63% (17/27) and partial concordance in 37% (10/27) of samples. OGM detected 76% (52/68) of the total SVs correctly (concordance rate for each type of SVs: aneuploidies, 83% [15/18]; balanced translocation, 80% [12/15] unbalanced translocation, 54% [7/13] deletions, 81% [13/16]; duplications, 100% [2/2] inversion 100% [1/1]; insertion, 100% [1/1]; marker chromosome, 0% [0/1]; isochromosome, 100% [1/1]). Sixteen discordant results were attributed to the involvement of centromeric/telomeric regions, detection sensitivity, and a low mapping rate and coverage. OGM identified additional SVs, including submicroscopic SVs and novel fusions, in five cases.

Conclusions: OGM shows a high level of concordance with conventional diagnostic methods for the detection of SVs and can identify novel variants, suggesting its potential utility in enabling more comprehensive SV analysis in routine diagnostics of hematologic malignancies, although further studies and improvements are required.

Key Words: Copy number variations, Gene fusion, Hematologic neoplasms, Optical genome mapping, Structural variations

Shim Y, et al.
Optical genome mapping in hematologic malignancies

ANNALS OF
LABORATORY
MEDICINE

INTRODUCTION

In oncology, molecular profiling of tumors provides vital information for diagnosis and treatment. Among various somatic molecular aberrations, structural variants (SVs) in chromosomes play important roles in tumor development and progression. Notably, in hematologic malignancies, a primary mechanism of oncogenesis is the formation of fusion genes by chromosomal rearrangements, resulting in loss of control over cell division and proliferation [1]. Therefore, SVs are important markers for diagnosis, therapy selection, and predicting prognosis through risk stratification in hematologic malignancies [2].

SVs are largely composed of unbalanced copy number variants (CNVs) (i.e., insertions, duplications, and deletions) and balanced rearrangements (i.e., inversions and translocations), with sizes ranging from 50 bp to over megabase pairs [3]. Conventional tests, including chromosomal banding analysis (CBA), FISH, chromosomal microarray (CMA), reverse transcription PCR (RT-PCR), and multiplex ligation-dependent probe amplification (MLPA), are performed in combination to detect these SVs. However, these tests have limitations. CBA has a low resolution, requires fresh samples, and involves a 7–10-day processing time because of the mandatory cell culturing process. For FISH and RT-PCR, probes and primers target known variants and cannot detect novel variants or rare breakpoints. These methods are also labor-intensive and lack multiplexing capacity. Despite its high resolution and capability to test the whole genome, CMA cannot detect balanced chromosomal aberrations and determine where an insertion has occurred when copy numbers increase.

Next-generation sequencing (NGS) has recently been adopted to identify genetic variants, including SVs, in hematologic malignancies [4-6]. However, its common short-read platform, with a read length of 150–300 bp, has limitations in precisely analyzing large SVs and homologous elements such as repetitive sequences and pseudogenes [7].

There is growing interest in optical genome mapping (OGM), a single-molecule strategy that can analyze tens to hundreds of kilobase-long reads, as a potential alternative technology for analyzing SVs [3, 8]. In OGM, fluorescent markers are used to tag particular sequences within DNA fragments of up to 1 megabase in length. This technique enables de novo assembly and gap filling and can detect SVs of up to tens of kilobases long [9-11]. Differences in the fluorescent labeling patterns relative to a consensus genome map are used to identify SVs [12]. OGM has the potential to overcome the limitations of conventional meth-

ods and detect SVs with a higher resolution in a substantially shorter time. Moreover, OGM can help identify novel chromosomal aberrations that may be used as additional markers for diagnosis, targeted therapy, and prognosis prediction.

We analyzed OGM results of diagnostic samples from patients with hematologic malignancies and evaluated their concordance with the results of conventional methods in detecting SVs. Several recent studies have assessed the clinical usefulness of SV detection using OGM in patients with blood cancer [13-21]. These studies mainly used CBA, FISH, RT-PCR, CMA, or MLPA as conventional methods for comparison. However, studies using RNA sequencing as a method for comparison, like our study, are scarce [20]. In particular, our study is the first report to assess the feasibility of OGM for SV detection in hematologic malignancies in Korea.

MATERIALS AND METHODS

Clinical samples

Residual bone marrow aspirate (BMA) samples of patients who underwent bone marrow examination to diagnose hematologic malignancies between July 2020 and April 2021 were included in this study. Clinical samples in which SVs were detected using conventional methods were retrospectively selected and evaluated using OGM. One sample (S18) was included to confirm a false-positive call identified using the RNA fusion panel. The Institutional Review Board of Severance Hospital in Seoul, Korea, approved this study (IRB No. 4-2020-0586) and waived the requirement for informed consent.

Conventional diagnostic methods

Conventional diagnostic methods were performed prior to this study as part of the routine diagnostic process, using standard procedures according to the manufacturers' instructions. For CBA, G-banding using Giemsa stain was conducted on cultured bone marrow cells. The karyotype was described following the International System for Human Cytogenetic Nomenclature [22]. FISH analysis was performed using commercially available Metasystems probes (Metasystems GmbH, Altlussheim, Germany) and Vysis probes (Abbott Molecular, Abbott Park, IL, USA).

For the RNA fusion panel and RT-PCR, total RNA was extracted from BMA samples using a QIAamp RNA Blood Mini Kit (Qiagen, Hilden, Germany). The RNA fusion panel test was performed as previously described [23, 24]. In brief, a target-enriched cDNA library was prepared using an Archer FusionPlex Pan-Heme kit (ArcherDX, Boulder, CO, USA). The library was amplified and puri-

ANNALS OF
LABORATORY
MEDICINE

Shim Y, et al.
Optical genome mapping in hematologic malignancies

fied, and the final products were sequenced using a NextSeq 550Dx system (Illumina, San Diego, CA, USA) and analyzed using the Archer Analysis Software (version 5.1, ArcherDX). For RT-PCR, cDNA was synthesized using a Transcriptor First Strand cDNA Synthesis Kit (Roche Diagnostics, Indianapolis, IN, USA). Multiplex RT-PCR was performed using a HemaVision 28N kit (DNA Diagnostic, Risskov, Denmark), which targets 28 translocations with 145 breakpoints.

Large genic or exonic CNVs identified by OGM were confirmed via CNV analysis using a target NGS panel that targets 531 genes related to hematologic malignancies (Dxome, Seoul, Korea), according to a previously described method [25, 26]. For gene CNV analysis, ExomeDepth and a custom tool were used [27, 28]. For chromosomal copy number analysis, off-target analysis was conducted using CopywriteR version 2.9.0 (Netherlands Cancer Institute, Amsterdam, Netherlands) [29].

OGM

Ultra-high molecular weight (UHMW) genomic DNA (gDNA) was isolated from white blood cells in heparinized BMA samples using a BMA DNA Isolation kit (Bionano Genomics, San Diego, CA, USA). The isolated UHMW gDNA was labeled with a DLS (Direct Label and Stain) DNA Labeling Kit (Bionano Genomics). All procedures were performed according to the manufacturer's instructions. The labeled UHMW gDNA was processed using a Bionano Genomics Saphyr system. Variant calling (SV and CNV detection) was executed using *de novo* assembly and variant annotation pipelines in Bionano Tools version 1.5.3. Variants were detected through comparison with the human reference genome (hg19). Annotated variants were further evaluated using a filtering strategy combining manufacturer default filtering and user filtering. Manufacturer default filtering was conducted using the filters embedded in the Bionano algorithm, according to the following criteria: 1) CNVs with ≥500 kb width and ≥0.99 confidence score were included; 2) SVs with a self-molecule count <5 were excluded. Variants that passed the criteria were subjected to subsequent analysis user filtering based on the following criteria: 3) SVs with a >0.01 population frequency in the Bionano control database were eliminated; 4) SVs (only insertions and deletions) with a <0.9 confidence score were filtered out (Supplemental Data Table S1). Four peripheral blood samples from patients without hematologic malignancies were included as negative controls.

Comparison of OGM and conventional diagnostic method results

SVs detected by OGM and conventional methods (including karyotyping, FISH, RT-PCR, and RNA fusion panel analysis) were compared to evaluate their concordance. When OGM detected all variants identified using conventional methods, the results were considered concordant. As OGM provides a higher resolution, there may be a slight difference in breakpoints, and corresponding variants were considered concordant when the assigned breakpoints were within the same chromosome arm. When OGM detected only a portion of the variants identified using the conventional methods, it was considered partial concordance. To confirm unique additional findings by OGM, we reviewed NGS CNV analysis results when available and performed additional tests when necessary.

RESULTS

Samples

In total, 27 BMA samples of hematologic malignancies, including AML (N=9), acute promyelocytic leukemia (APL; N=1), CML in the chronic phase (CML-CP; N=3), primary myelofibrosis (PMF; N=1), MDS with excess blasts-2 (MDS-EB-2; N=1), MDS with single lineage dysplasia (MDS-SLD; N=1), B-lymphoblastic leukemia (B-ALL; N=6), CLL (N=1), marginal zone B-cell lymphoma (MZBCL; N=1), lymphoplasmacytic lymphoma (LPL; N=1), and plasma cell myeloma (PCM) (N=2), were analyzed. The median age of the study cohort was 55 yrs (range: 3–84 yrs); 13 samples were from men, and 14 were from women. The 27 samples were analyzed using conventional methods, including karyotyping (27/27), FISH (7/27), RT-PCR (11/27), and RNA fusion panel analysis (14/27).

Samples were classified into simple or complex cases based on the number of SVs detected using the conventional methods (simple: 0–2; complex: ≥3). Of the 27 cases, 18 were classified as simple and nine as complex. In total, 68 SVs (18 aneuploidies, 28 translocations, 16 deletions, two duplications, one inversion, one insertion, one marker chromosome, and one isochromosome) were detected.

OGM data quality

OGM of the 27 samples resulted in an average DNA amount of 1,220.8 Gbp, an average 234.65-fold effective coverage, an average N50 of 0.208 Mbp, an average label density of 15.24/100 kb, and an average mapping rate of 60.2%. For *de novo* assembly for SV analysis, the minimum recommended cov-

Shim Y, et al.
Optical genome mapping in hematologic malignancies

ANNALS OF
LABORATORY
MEDICINE

erage for detecting heterozygous and homozygous SVs is 80×. Twenty-six of the 27 samples met this recommendation, and the results of all samples were compared with those from the conventional methods. The data quality of all cases is provided in Supplemental Data Table S2. No SVs were detected by OGM in the four negative controls.

OGM in simple cases

In the 18 simple cases (seven AML, one APL, three CML-CP, one PMF, five B-ALL, and one CLL), the conventional methods detected no SVs in one case, one in 14 cases, and two in three cases (Table 1), totaling 20 SVs. OGM detected 17 (85%) SVs correctly, only part of the aberration in the three remaining (15%) SVs, and 10 additional SVs. Overall, OGM showed concordance in 15 (83.3%) cases and partial concordance in three (16.7%) cases. In the 15 concordant cases, in which OGM could detect all variants identified using conventional methods, five cases also had additional SVs detected uniquely by OGM.

The three simple cases that showed partial concordance were S12, S13, and S14. Cases S12 and S13 were CML-CP cases with complex translocations, harboring four-break and three-break translocations, respectively. In S12, t(3;11;9;22) (p21;q13;q34;q11.2) was reported by CBA but missed by OGM [t(3;11)(p21;q13)]. Similarly, t(7;9;22)(q22;q34;q11.2) was reported by CBA in S13, but t(7;9)(q22;q34) was missed by OGM. For S14, a case of PMF, der(6)t(1;6)(q21;p21) was reported by CBA, whereas OGM missed t(1;6)(q21;p21) and 1q21q44 gain.

Additional findings by OGM in simple cases

OGM revealed additional findings in five simple cases: S4, S11, S17, S18, and S21. S4 was an AML case; S11 was a CML-CP case; and S17, S18, and S21 were B-ALL cases. The karyotyping result of S4 was initially reported as 46,XX,ins(9)(q13p13p24) [22]/46,XX[1] or 46,XX,ins(9)(q13q21q13)[22]/46,XX[1]. OGM revealed a *MYC* amplification as the inserted component, which was confirmed using FISH and NGS CNV analyses (Fig. 1). Based on this, we modified the karyotyping result as 46,XX, der(9)ins(9;8)(q13;q22q24.2)[22]/46,XX[1]. In S11, in addition to the three translocations associated with the three-break balanced translocation and the *BCR::ABL1* fusion detected using conventional methods, OGM identified the *ARL2-SNX15::CABIN1* fusion. In S17, OGM correctly detected t(9;22)(q34;q11.2) *BCR::ABL1* fusion and trisomy 21 identified using the conventional methods and further detected *SETD2* exon 1–10 deletion. NGS CNV analysis results were reviewed to confirm the new finding, and *SETD2* exon 2–9 deletion and *IKZF1* exon 4–7 de-

letion were detected. The *IKZF1* exon 4–7 deletion, which was not called by OGM and was likely missing from the OGM results, was detected upon manual inspection of the OGM profile. For S18, CBA revealed a normal karyotype, and a false-positive call for the *ATP5L::KMT2A* fusion was reported by the RNA fusion panel. The *ATP5L::KMT2A* fusion was confirmed as a false positive by RT-PCR. OGM results confirmed the false-positive call of *ATP5L::KMT2A* and found additional variants of del(12) (p13.31p12.1), del(17)(p11.2p13.3), dup(17)(p11.2q25.3), and *EP300::ZNF384* fusion. *EP300::ZNF384* was confirmed using Sanger sequencing, and del(12)(p13.31p12.1), del(17) (p11.2p13.3), and dup(17)(p11.2q25.3) were confirmed using NGS CNV analysis (Fig. 2). In S21, OGM additionally identified *CDKN2A* and *CDKN2B* whole gene deletions, and NGS CNV results confirmed *CDKN2A* whole gene deletion, *CDKN2B* exon 2 deletion, and *IKZF1* exon 4–7 deletion. Notably, the deletion of *IKZF1* exon 4–7, which was not called by OGM, was detectable upon manual inspection of the OGM profile, as in the case of S17.

OGM in complex cases

In the nine complex cases (two AML, one MDS-EB-2, one MDS-SLD, one B-ALL, one MZBCL, one LPL, and two PCM), conventional methods detected three to 11 SVs in each case, totaling 48 SVs (Table 2). OGM accurately detected 35 (72.9%) SVs, partially identified four SVs (8.3%), and failed to detect nine (18.8%) SVs. Overall, OGM demonstrated concordance in two (22%) cases and partial concordance in seven (78%).

In two of the complex cases with partial concordance (S15 and S26), OGM failed to correctly detect SVs involving centromeric regions. Specifically, in S15, OGM accurately identified all three aneuploidies but missed the t(1;10)(q21;q11.2) associated with the derivative chromosome 10. Similarly, in S26, OGM accurately detected six deletions, two aneuploidies, one translocation, and an *IGH::FGFR3* rearrangement but missed the t(12;18)(p11.2;p11.2) associated with the pseudodicentric chromosome 12. In another partially concordant complex case, S20, OGM failed to correctly detect SVs involving the telomeric region, specifically missing a microdeletion in the telomeric region of Xp22.33 and the *P2RY8::CRLF2* fusion resulting from the microdeletion, identified only using the RNA fusion panel. This microdeletion was not captured during routine diagnostic testing using NGS CNV analysis.

In three other complex cases, S16, S25, and S27, OGM failed to correctly detect SVs in minor subclones. In S16, two deletions were detected correctly, whereas t(2;14)(q35;q13) and 14q13q32 gain

Table 1. Comparison of routine diagnostic test results with OGM results in simple cases

Sample ID	Diagnosis	Karyotype	FISH	RT-PCR/RNA fusion	OGM results (SV tool and/or CNV tool)	Summary
2	AML	46,XX[20]	NA	NUP98::NSD1	t(5;11)(q35.3;p15.4) NUP98-NSD1	Concordant
3	AML	46,XY,inv(16)(p13q22)[23]/46,XY[2]	NA	CBFB::MYH11	t(16;16)(p13.11;q22.1) CBFB-MYH11	Concordant
4	AML	46,XX,der(9)ins(9;8)(q13;q22q24.2)[22]/ 46,XX[1]	NA	NA	MYC amplification	Concordant Additional by OGM*
5	AML	47,XX,+8,t(9;11)(p21;q23)[20]	NA	KMT2A::MLLT3	+8, t(9;11)(p21.3;q23.3) KMT2A-MLLT3	Concordant
6	AML	46,XX,t(11;12)(p15;q13)[20]	NA	NUP98::HOXC13	t(11;12)(p15.4;q13.13) NUP98-HOXC13	Concordant
8	AML	46,XY,dup(19)(p13.1p13.3)[20]/46,XY[6]	NA	Negative	dup(19)(p13.2p13.2)	Concordant
9	AML	46,XX,t(6;9)(p22;q34)[16]/46,XX[4]	NA	DEK::NUP214	t(6;9)(p22.3;q34.13) DEK-NUP214	Concordant
10	APL	46,XY,t(15;17)(q24;q21)[19]/46,XY[1]	NA	PML::RARA	t(15;17)(q24.1;q21) PML-RARA	Concordant
11	CML-CP	46,XY,t(9;22;11)(q34;q11.2;q13)[20]	NA	BCR::ABL1 (b3a2, major type)	t(9;22)(q34.12;q11.23) BCR-ABL1 t(11;22)(q13.1;q11.23) ARL2-SNX15-CABIN1 t(9;11)(q34.11;q13.1)	Concordant Additional by OGM
12	CML- CP	46,XX,t(3;11;9;22)(p21;q13;q34;q11.2)[20]	NA	BCR::ABL1 (b2a2, major type)	t(9;11)(q34.11;q13.2) t(9;22)(q34.12;q11.23) t(3;22)(p21.31;q11.23)	Partial concordance
13	CML-CP	46,XY,t(7;9;22)(q22;q34;q11.2)[14]	NA	BCR::ABL1 (b2a2, major type) BCR::ABL1 (e1a2, minor type, weakly positive)	t(7;22)(q22.1;q11.23) t(9;22)(q34.12;q11.23)	Partial concordance
14	PMF	46,XY,der(6)t(1;6)(q21;p21)[3]/46,XY[17]	NA	NA	del(6)(p21.1p25.3)	Partial concordance
17	B-ALL	46,XY,t(9;22)(q34;q11.2)[3]/ 47,idem,+21[9]/46,XY[8]	NA	BCR::ABL1 (e1a2, minor type)	t(9;22)(q34.12;q11.23) BCR-ABL1 +21 IKZF1 exon 4-7 deletion† SETD2 exon 1-10 deletion	Concordant Additional by OGM‡
18	B-ALL	46,XY[30]	Negative for t(11q23) break-apart	Negative§	del(12)(p13.31p12.1) del(17)(p11.2p13.3) dup(17)(p11.2q25.3) t(12;22)(p13.31;q13.2) EP300-ZNF384	Concordant Additional by OGM‖,¶
19	B-ALL	47,XX,+X,t(2;14)(p11.2;q32)[5]/46,XX[20]	NA	Negative for BCR::ABL1	+X, t(2;14)(p11.2;q32.33)	Concordant
21	B-ALL	46,XY,t(2;12)(p11.2;p13)[5]/46,XY[4]	NA	Negative for BCR::ABL1	t(2;12)(p12;p13.2) IKZF1 exon 4-7 deletion† CDKN2A whole gene deletion CDKN2B whole gene deletion	Concordant Additional by OGM**
22	B-ALL	46,XY[13]	NA	ETV6::RUNX1	t(12;21)(p13.2;q22.12)	Concordant
23	CLL	46,XY[20]	Positive for del(13q)	NA	del(13)(q14.3)	Concordant

*Detection of MYC amplification by OGM was confirmed by FISH.
†IKZF1 exon 4–7 deletion was not called by OGM but was detectable upon manual inspection.
‡Detection of SETD2 exon 1–10 deletion by OGM was confirmed using NGS CNV analysis.
§A false-positive call (ATP5L-KMT2A fusion) was initially called using an RNA fusion panel.
‖Detection of the EP300-ZNF384 fusion by OGM was confirmed by Sanger sequencing.
¶Detection of del(12)(p13.31p12.1), del(17)(p11.2p13.3), and dup(17)(p11.2q25.3) by OGM was confirmed by NGS CNV analysis.
**Detection of CDKN2A and CDKN2B whole gene deletion by OGM was confirmed by NGS CNV analysis.
Abbreviations: OGM, optical genome mapping; FISH, fluorescence in situ hybridization; RT-PCR, reverse transcription PCR; SV, structural variant; CNV, copy number variant; APL, acute promyelocytic leukemia; B-ALL, B-lymphoblastic leukemia; CML-CP, chronic myeloid leukemia in chronic phase; PMF, primary myelofibrosis; NA, not available.
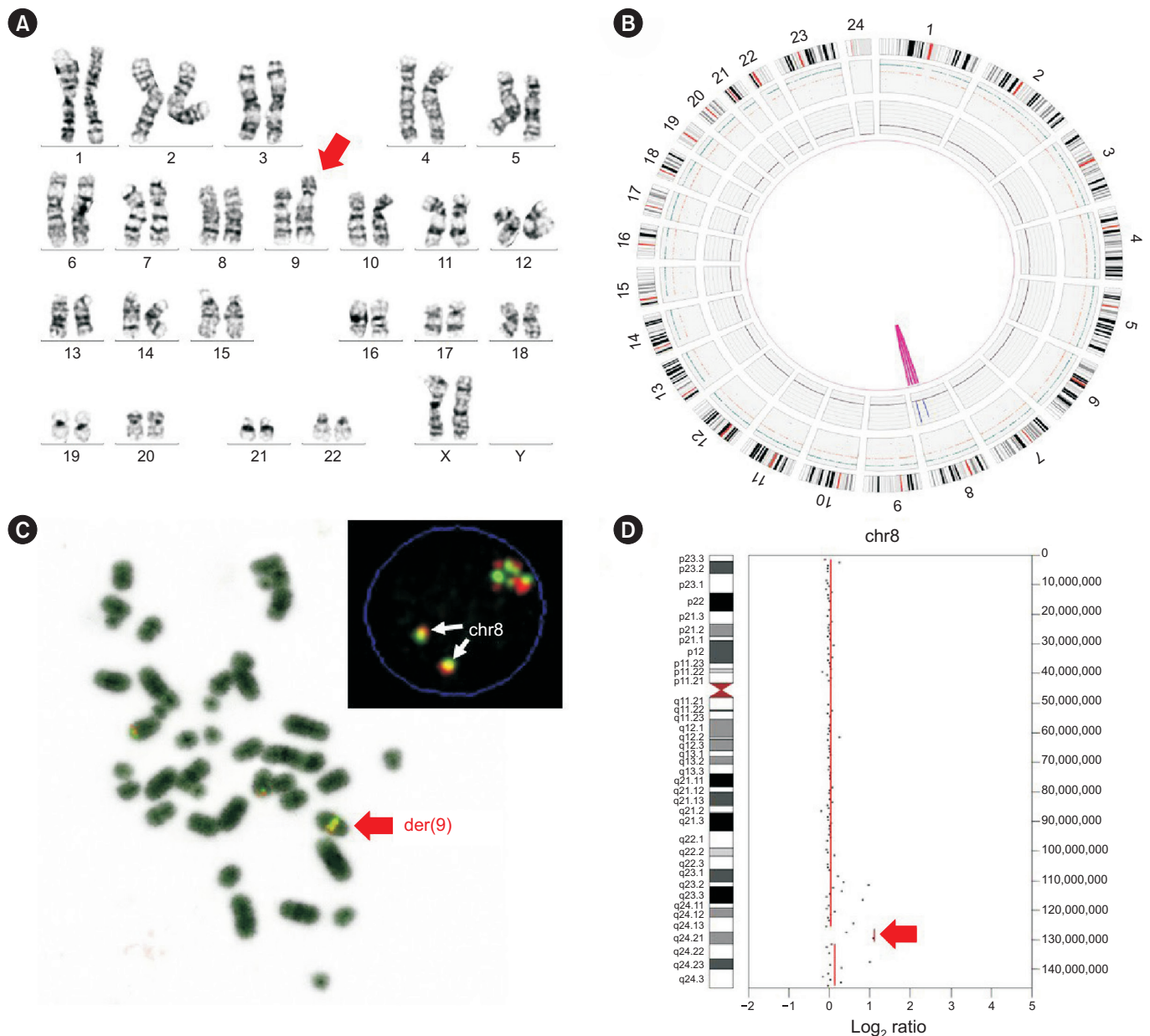
Fig. 1. Results of conventional laboratory tests and OGM for S4. (A) CBA revealed an insertion in the long arm of chromosome 9. (B) Whole-genome circos plot obtained by OGM showing *MYC* amplification. (C) FISH was performed using Vysis probes (Abbott Molecular). (D) NGS CNV analysis showing amplification of the q24.21 band in chromosome 8.
Abbreviations: OGM, optical genome mapping; CBA, chromosomal banding analysis; chr, chromosome; CNV, copy number variant.

associated with derivative chromosome 2, loss of chromosome 14, and del(13)(q13q22) were missed by OGM. These SVs were observed in only 16% (3/19 cells) of cases in CBA. In S25, one deletion and a gain of isochromosome, found in 18/25 cells in CBA, were accurately identified by OGM. However, OGM failed to detect one deletion that was identified in the minor subclone comprising 28% (7/25 cells) of cases in CBA. In S27, OGM correctly detected one unbalanced translocation and one aneu-

ploidy, but missed two translocations, t(X;6)(p11.2;p25) and t(11;14)(q13;q32), and the *IGH::CCND1* rearrangement. These SVs were part of the composite karyotype, which constituted 17.5% (7/40 cells) of cases in CBA. Finally, in one complex case (S24), only one balanced translocation was correctly detected by OGM, whereas loss of chromosomes 17 and X, gain of der(6;9) (p10;p10), and a marker chromosome were all undetected by both OGM and NGS CNV analysis, leading to a notable discrep-
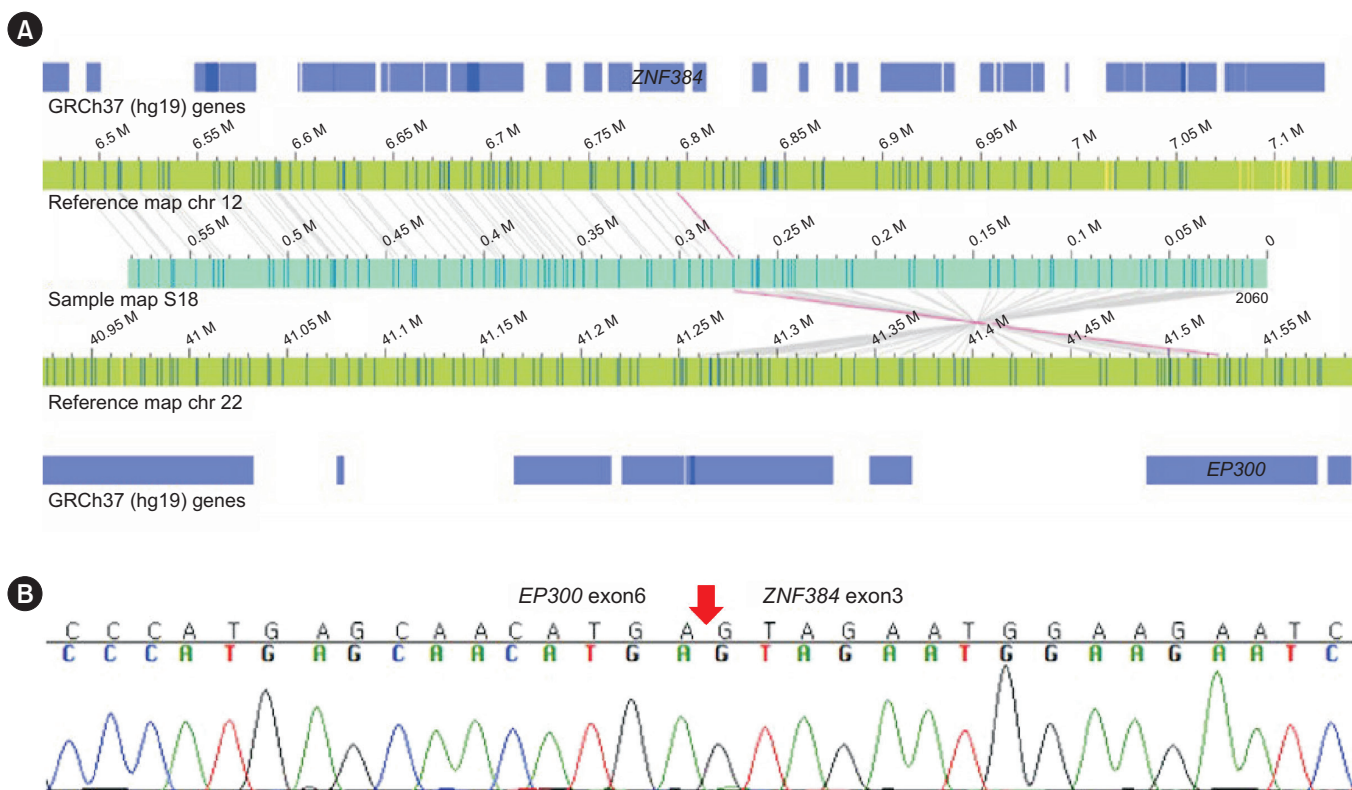
ANNALS OF LABORATORY MEDICINE

Shim Y, et al.
Optical genome mapping in hematologic malignancies

Fig. 2. Additional finding of *EP300::ZNF384* fusion by OGM in S18. (A) Genome map view showing the *EP300::ZNF384* fusion. Map of S18 (blue) aligned to reference maps of chromosome 12 and chromosome 22 (green), with breakpoints in *ZNF384* and *EP300*, respectively. Label alignments between the reference and sample genome maps are indicated by gray lines. Translocation breakpoints are indicated by pink lines. (B) Confirmation of the *EP300::ZNF384* fusion using Sanger sequencing. The red arrow indicates the breakpoint.
Abbreviations: OGM, optical genome mapping; chr, chromosome.

ancy as these SVs were observed in a substantial proportion of cells (i.e., 61% [11/18 cells]) in CBA.

DISCUSSION

We analyzed SVs in various hematologic malignancies using OGM and compared the results with those of routine diagnostic tests (CBA, FISH, RT-PCR, and an RNA fusion panel) to investigate their concordance. Overall, OGM showed concordance in 63% (17/27) of cases and partial concordance in 37% (10/27), with no cases of non-concordance. OGM correctly identified 76% (52/68) of total SVs, with specific concordance rates for each type of aberration as follows: aneuploidies (83% [15/18]), balanced translocations (80% [12/15]), unbalanced translocations (54% [7/13]), deletions (81% [13/16]), duplications (100% [2/2]), inversion (100% [1/1]), insertion (100% [1/1]), marker chromosome (0% [0/1]), and isochromosome (100% [1/1]). Compared with previously published results [30], we observed a relatively low concordance rate, especially in complex cases.

OGM showed limitations by detecting only part of the SVs or entirely missing some SVs. We analyzed the possible reasons for all discordant results and found they could be summarized as follows: i) SVs involving centromeric and/or telomeric regions, ii) SVs in minor subclones with low frequency likely below the detection sensitivity, and iii) SVs in samples with low mapping rate and coverage (Table 3).

Highly repetitive regions, such as centromeric regions, short arms of acrocentric chromosomes, pseudo-autosomal regions (PARs), and telomeric regions, are often poorly covered by OGM because of missing labels and unreliable reference map data. Consequently, OGM may fail to detect SVs involving these regions, a well-known limitation [14-17]. However, as these regions may contain clinically relevant SVs, efforts should be undertaken to identify recurrent SVs in these areas. For instance, a microdeletion in the PAR of Xp22.33 and the *P2RY8::CRLF2* fusion caused by the microdeletion were missed by OGM in S20. A similar detection failure has been reported previously [18]. Studies have reported *P2RY8::CRLF2* as a recurrent rearrangement in

Shim Y, et al.
Optical genome mapping in hematologic malignancies

ANNALS OF
LABORATORY
MEDICINE

Table 2. Comparison of routine diagnostic test results with OGM results in complex cases

Sample ID	Diagnosis	Karyotype	FISH	RT-PCR/ RNA fusion	OGM results (SV tool and/or CNV tool)	Summary
1	AML	46,XY,del(5)(q13q31),del(7)(q11.2),+11, der(12)t(1;12)(p13;q24.3), ?psu dic(17;16)(p11.2;q21), ?der(18)t(18;19)(q23;q13.1-13.3)[20]	NA	Negative	del(5)(q14.3q34), del(7)(q11.23), +11, t(1;12)(p13.3;q24.33), t(17;16)(p11.2;q21), t(18;19) (q23;q13.2)	Concordant
7	AML	45,XX,del(11)(q14q24), -16,der(21)t(16;21)(p11;q22)[20]	NA	*FUS-ERG*	del(11)(q14.1q24.1), -16, t(16;21)(p11.2;q22.2) *FUS-ERG*	Concordant
15	MDS-EB-2	48,XY,+8,+der(10)t(1;10)(q21;q11.2)[4] /49,sl,+9[14]/50,sdl1,+6[4]/46,XY[2]	Positive for trisomy 8	Negative	+8, dup(1)(q21.1q44), dup(10) (p11.1p15.3), dup(10)(q11.2) +9, +6	Partial concordance
16	MDS-SLD	45,XX,der(2)t(2;14)(q35;q13),del(5)(q14), del(11)(q14),del(13)(q13q22),-14[3]/46,XX[16]	NA	NA	del(2)(q35q37.3), del(5)(q31.1), del(11)(q12.2)	Partial concordance
20	B-ALL	48-52,XX,dup(1)(q32q21),+4,+6,+9, +der(14)t(14;21)(q21.1;q21.2),+21,+21[cp6] /46,XX[29]	NA	*P2RY8-CRLF2* Negative for *BCR-ABL1*	dup(1)(q31.3q21.2), +4, +6, +9, +21, +21, t(14;21)(q21.1;q21.2), dup(14)(q11.2q21.1), dup(21) (q21.2q22.3)	Partial concordance
24	MZBCL	46,X,-X,t(3;7)(q27;q32),?+der(6;9)(p10;p10), -17,+mar[11]/46,XX,t(3;7)[4]/46,XX[3]	NA	NA	t(3;7)(q27.2;q32.2)	Partial concordance
25	LPL	47,XX,+i(5)(p10),del(7)(q32)[18] /47,idem,del(16)(q22)[7]	Negative for del(17p), del(11q), and del(13q)	NA	+i(5)(p10), del(7)(q31.32q36.1)	Partial concordance
26	PCM	43,X,der(X)t(X;3)(p11.4;q13.1), del(1)(p21p31),del(2)(q24q32), del(4)(p15.1p15.3), psu dic(12)t(12;18)(p11.2;p11.2), -13,del(14)(q21q31),del(20)(p11.2), -22[5]/46,XX[15]	Positive for del(17p) and t(4;14) Negative for t(11;14) and t(14;16)	NA	t(3;X)(q13.13;p11.4), dup(3) (q13.13q29), del(X) (p11.4p22.33), del(1) (p21.1p31.1), del(2) (q24.1q32.1), del(4) (p15.1p15.33), del(12) (p12.1p13.33), del(18) (p11.22p11.32), -13, del(14) (p21.3p31.3), t(4;14) (q16.3;q32.33), del(20)(p11.2), -22, del(17)(p13.1)	Partial concordance
27	PCM	45,X,t(X;6)(p11.2;p25), der(14)t(11;14) (q13;q32), der(18)t(18;21)(q22;q21),-21[cp7] /46,XX[33]	Positive for t(11;14) Negative for del(17p), t(4;14), and t(14;16)	NA	t(18;21)(q22.3;q21.1), del(18)(q22.3q23), del(21)(q21.1q21.3), dup(11)(q13.4q23.1)	Partial concordance

Abbreviations: OGM, optical genome mapping; FISH, fluorescence *in situ* hybridization; RT-PCR, reverse transcription PCR; SV, structural variant; CNV, copy number variant; B-ALL, B-lymphoblastic leukemia; LPL, lymphoplasmacytic lymphoma; MDS-EB-2, myelodysplastic syndrome with excess blasts-2; MDS-SLD, myelodysplastic syndrome with single lineage dysplasia; MZBCL, marginal zone B-cell lymphoma; PCM, plasma cell myeloma; NA, not available.

B-ALL that is associated with distinctive features and poor prognosis and may influence treatment choice [31-33]. The detection failure of recurrent SVs that have clinical significance by OGM is a critical problem that must be resolved.

For undetected SVs present in minor subclones in four cases (S14, S16, S25, and S27), we attribute the discrepancy to the detection sensitivity of OGM. These SVs were detected in a median of 16.75% of cells by CBA (range: 15%–28%). While OGM missed these subclonal SVs, it detected other SVs present in the same subclone. Additionally, some SVs were identified in only 15%–20% of cells using CBA among the concordant cases, indicating inconsistent detection sensitivity of OGM with respect to CBA results. Similar results have been reported previously [16], and Rack, *et al.* [14] additionally performed interphase FISH and established that OGM detected SVs present in at least 15% of cells. However, we could not perform additional interphase FISH on these cases owing to a lack of samples.

For samples with discordant results attributed to a low map-

ANNALS OF
LABORATORY
MEDICINE

Shim Y, et al.
Optical genome mapping in hematologic malignancies

Table 3. Structural variations missed by OGM and probable cause of detection failure

Sample ID	Diagnosis	Structural variations missed by OGM	Possible explanation for discordant results	Comment
12	CML-CP	t(3;11)(p21;q13)	Low map rate and coverage (map rate 24.5%, coverage 99.11×)	
13	CML-CP	t(7;9)(q22;q34)	Involvement of telomeric region	
14	PMF	t(1;6)(q21;p21), gain of 1q21q44	Detection sensitivity	Detected in 15% (3/20) of cells in CBA
15	MDS-EB-2	t(1;10)(q21;q11.2)	Involvement of centromeric region	
16	MDS-SLD	t(2;14)(q35;q13), gain of 14q13q32, monosomy 14, del(13)(q13q22)	Detection sensitivity or low map rate and coverage (map rate 28.4%, coverage 87.75 X)	Detected in 16% (3/19) of cells in CBA
20	B-ALL	Microdeletion in Xp22.33	Involvement of telomeric region	
24	MZBCL	Monosomy 17, monosomy X, +der(6;9)(p10;p10), marker chromosome	Low map rate and coverage (map rate 38.9%, coverage 98.85 X)	Not detected by NGS CNV
25	LPL	del(16)(q22)	Detection sensitivity	Detected in 28% (7/25) of cells in CBA
26	PCM	t(12;18)(p11.2;p11.2)	Involvement of centromeric region	
27	PCM	t(X;6)(p11.2;p25), t(11;14)(q13;q32)	Detection sensitivity	Detected in 17.5% (7/40) of cells in CBA

Abbreviations: OGM, optical genome mapping; B-ALL, B-lymphoblastic leukemia; CML-CP, chronic myeloid leukemia in chronic phase; PMF, primary myelofibrosis; LPL, lymphoplasmacytic lymphoma; MDS-EB-2, myelodysplastic syndrome with excess blasts-2; MDS-SLD, myelodysplastic syndrome with single lineage dysplasia; MZBCL, marginal zone B-cell lymphoma; PCM, plasma cell myeloma.

ping rate and coverage, the mapping rate was below 60%, and coverage was below 100×. Many other samples had a mapping rate below 60%, but the distinguishing factor was coverage. Other samples with a low mapping rate had a coverage above 100× (median 174.16×, range: 102.65–277.26×), whereas the discordant samples had a coverage below 100× (median 98.85×, range: 87.75–99.11×). This aligns with the Bionano Molecule Quality Report Guidelines that state that when the obtained mapping rate is significantly lower than the minimum desired mapping rate (i.e., <60%), extra depth can compensate for the low mapping rate. However, there was one exceptional case (S5) where OGM correctly identified all SVs despite a low mapping rate and low coverage.

Overall, the largest number of missed SVs per sample was four for samples S16 and S24. For S16, there are two possible explanations for the discordant OGM results: detection sensitivity or low mapping quality. Although S24 can be classified as a discordant case attributable to a low mapping rate and coverage, the SVs detected using CBA may represent a culture selection bias because, similar to the OGM results, NGS CNV results revealed no SVs.

Despite the aforementioned limitations, OGM demonstrated many advantages in detecting SVs. First, OGM was able to detect different types of SVs simultaneously in a single test in many cases. Second, OGM clarified the boundaries/breakpoints of SVs observed in CBA owing to its higher resolution. Third,

OGM identified *IGH* rearrangements even when they did not result in chimeric transcripts. We included two PCM cases, S26 and S27, to assess the capability of OGM to identify these rearrangements, which are challenging to detect using RNA sequencing. OGM successfully detected *IGH::FGFR3* in S26 but failed to detect *IGH::CCND1* in S27. The detection failure in S27 was probably attributed to detection sensitivity, as mentioned earlier. For a reliable and accurate conclusion, more cases must be examined. Fourth, OGM found additional SVs, including submicroscopic SVs and novel gene fusions with potential clinical significance. In AML case S4, OGM revealed that the inserted segment in chromosome 9 was a *MYC* amplification, which implies a poor prognosis in AML [34]. In B-ALL case S18, OGM newly detected del(12)(p13.31p12.1), del(17)(p11.2p13.3), dup(17)(p11.2q25.3), and *EP300::ZNF384* fusion. In a previous study, *EP300::ZNF384* was detected only by OGM in a B-ALL case [14], and this aberration may influence the clinical outcome of B-ALL [35]. In B-ALL cases S17 and S21, *SETD2*, *CDKN2A/B*, and *IKZF1* deletions were discovered by OGM, and all of these submicroscopic deletions have the potential to influence risk stratification, prognosis prediction, and patient management. *SETD2* deletions have been identified in various leukemias, and its loss has been associated with chemotherapy resistance [36]. Similarly, *IKZF1* deletions are emerging as an important prognostic biomarker and are associated with resistance to tyrosine kinase inhibitors in B-ALL. Co-occurring *CDKN2A/B* and *IKZF1*

deletions are associated with worse outcomes [37].

Collectively, our findings indicate that OGM can play a role in revealing many clinically significant SVs. Furthermore, in CML-CP case S11, OGM helped discover a novel gene fusion, *ARL2-SNX15::CABIN1*, which is a key strength of this technique. Identifying such fusions using OGM could pave the way for further investigations that may lead to clinically significant discoveries in the pathogenesis, diagnosis, prognosis, and treatment of hematological malignancies.

In addition to the intrinsic limitations of the OGM technology, this study had additional limitations. Its retrospective design is a primary limitation, and future studies with a prospective design are essential to validate the findings and establish the clinical utility of OGM. Moreover, the study assessed only a limited number of samples and variants, warranting future research involving larger cohorts with sufficient sample size and the analysis of a broader range of SVs for each specific hematologic malignancy diagnosis. Third, not all conventional methods (karyotyping, FISH, RT-PCR, and RNA fusion panel analysis) were consistently performed in all cases during routine diagnostic work-up, limiting the accuracy of the evaluation. A more comprehensive assessment could be achieved by consistently applying all conventional methods to every sample included in the study. Finally, as this study primarily focused on evaluating concordance, further studies are necessary to evaluate the performance characteristics of OGM, including sensitivity, specificity, and predictive values.

In conclusion, we assessed the concordance between OGM and traditional diagnostic methods for detecting SVs in hematologic malignancies, revealing a certain level of concordance. However, limitations were observed in detecting SVs involving centromeric and/or telomeric regions, minor subclones with low frequency, and samples with low mapping rates and coverage. Despite these limitations, OGM holds substantial value in identifying variants undetectable by conventional methods and discovering novel variants, suggesting its potential utility in comprehensively profiling SVs in routine diagnostics of hematologic malignancies. The identification of novel variants through OGM may yield clinically significant insights into the pathogenesis, diagnosis, prognosis, and treatment of hematological malignancies. However, for the implementation of OGM in clinical practice, further validation through prospective studies with larger cohorts and ongoing technical and analytical enhancements to address current limitations is imperative.

SUPPLEMENTARY MATERIALS

Supplementary materials can be found via https://doi.org/10.3343/alm.2023.0339

ACKNOWLEDGEMENTS

None.

AUTHOR CONTRIBUTIONS

Shim Y performed optical genome mapping analysis and wrote the manuscript; Koo YK collected patient data and wrote the manuscript; Shin S conceptualized, designed, supervised the study and reviewed and edited the manuscript; Lee ST, Lee KA, and Choi JR supervised the research and reviewed the manuscript. All authors have read and approved the final manuscript.

CONFLICTS OF INTEREST

None declared.

RESEARCH FUNDING

REFERENCES

1. Schütte J, Reusch J, Khandanpour C, Eisfeld C. Structural variants as a basis for targeted therapies in hematological malignancies. Front Oncol 2019;9:839.
2. Park MS, Kim HY, Lee JJ, Cho D, Jung CW, Kim HJ, et al. The first case of acute myeloid leukemia with t(10;11)(p13;q21);PICALM-MLLT10 rearrangement presenting with extensive skin involvement. Ann Lab Med 2023;43:310-4.
3. Ho SS, Urban AE, Mills RE. Structural variation in the sequencing era. Nat Rev Genet 2020;21:171-89.
4. Braggio E, Egan JB, Fonseca R, Stewart AK. Lessons from next-generation sequencing analysis in hematological malignancies. Blood Cancer J 2013;3:e127.
5. Merker JD, Valouev A, Gotlib J. Next-generation sequencing in hematologic malignancies: what will be the dividends? Ther Adv Hematol 2012;3:333-9.
6. He J, Abdel-Wahab O, Nahas MK, Wang K, Rampal RK, Intlekofer AM, et al. Integrated genomic DNA/RNA profiling of hematologic malignancies in the clinical setting. Blood 2016;127:3004-14.
7. Jain M, Koren S, Miga KH, Quick J, Rand AC, Sasani TA, et al. Nanopore sequencing and assembly of a human genome with ultra-long reads. Nat Biotechnol 2018;36:338-45.
8. Feuk L, Carson AR, Scherer SW. Structural variation in the human ge-

ANNALS OF LABORATORY MEDICINE

Shim Y, et al.
Optical genome mapping in hematologic malignancies

nome. Nat Rev Genet 2006;7:85-97.

9. Lam ET, Hastie A, Lin C, Ehrlich D, Das SK, Austin MD, et al. Genome mapping on nanochannel arrays for structural variation analysis and sequence assembly. Nat Biotechnol 2012;30:771-6.

10. Hastie AR, Dong L, Smith A, Finklestein J, Lam ET, Huo N, et al. Rapid genome mapping in nanochannel arrays for highly complete and accurate de novo sequence assembly of the complex Aegilops tauschii genome. PLoS One 2013;8:e55864.

11. Cao H, Hastie AR, Cao D, Lam ET, Sun Y, Huang H, et al. Rapid detection of structural variation in a human genome using nanochannel-based genome mapping technology. Gigascience 2014;3:34.

12. Chan S, Lam E, Saghbini M, Bocklandt S, Hastie A, Cao H, et al. Structural variation detection and analysis using Bionano optical mapping. Methods Mol Biol 2018;1833:193-203.

13. Neveling K, Mantere T, Vermeulen S, Oorsprong M, van Beek R, Kater-Baats E, et al. Next-generation cytogenetics: comprehensive assessment of 52 hematological malignancy genomes by optical genome mapping. Am J Hum Genet 2021;108:1423-35.

14. Rack K, De Bie J, Ameye G, Gielen O, Demeyer S, Cools J, et al. Optimizing the diagnostic workflow for acute lymphoblastic leukemia by optical genome mapping. Am J Hematol 2022;97:548-61.

15. Gerding WM, Tembrink M, Nilius-Eliliwi V, Mika T, Dimopoulos F, Ladigan-Badura S, et al. Optical genome mapping reveals additional prognostic information compared to conventional cytogenetics in AML/MDS patients. Int J Cancer 2022;150:1998-2011.

16. Puiggros A, Ramos-Campoy S, Kamaso J, de la Rosa M, Salido M, Melero C, et al. Optical genome mapping: a promising new tool to assess genomic complexity in chronic lymphocytic leukemia (CLL). Cancers (Basel) 2022;14.

17. Soler G, Ouedraogo ZG, Goumy C, Lebecque B, Aspas Requena G, Ravinet A, et al. Optical genome mapping in routine cytogenetic diagnosis of acute leukemia. Cancers (Basel) 2023;15.

18. Lestringant V, Duployez N, Penther D, Luquet I, Derrieux C, Lutun A, et al. Optical genome mapping, a promising alternative to gold standard cytogenetic approaches in a series of acute lymphoblastic leukemias. Genes Chromosomes Cancer 2021;60:657-67.

19. Sahajpal NS, Mondal AK, Tvrdik T, Hauenstein J, Shi H, Deeb KK, et al. Clinical validation and diagnostic utility of optical genome mapping for enhanced cytogenomic analysis of hematological neoplasms. J Mol Diagn 2022;24:1279-91.

20. Brandes D, Yasin L, Nebral K, Ebler J, Schinnerl D, Picard D, et al. Optical genome mapping identifies novel recurrent structural alterations in childhood *ETV6::RUNX1+* and high hyperdiploid acute lymphoblastic leukemia. Hemasphere 2023;7:e925.

21. Yang H, Garcia-Manero G, Sasaki K, Montalban-Bravo G, Tang Z, Wei Y, et al. High-resolution structural variant profiling of myelodysplastic syndromes by optical genome mapping uncovers cryptic aberrations of prognostic and therapeutic significance. Leukemia 2022;36:2306-16.

22. Shaffer LG, McGowan-Jordan J, Schmid M, eds. ISCN 2013: an international system for human cytogenetic nomenclature (2013). Basel: Karger Medical and Scientific Publishers, 2013.

23. Kim B, Kim E, Lee ST, Cheong JW, Lyu CJ, Min YH, et al. Detection of recurrent, rare, and novel gene fusions in patients with acute leukemia using next-generation sequencing approaches. Hematol Oncol 2020;38:82-8.

24. Kim B, Lee H, Shin S, Lee ST, Choi JR. Clinical evaluation of massively parallel RNA sequencing for detecting recurrent gene fusions in hematologic malignancies. J Mol Diagn 2019;21:163-70.

25. Kim B, Lee H, Kim E, Shin S, Lee ST, Choi JR. Clinical utility of targeted NGS panel with comprehensive bioinformatics analysis for patients with acute lymphoblastic leukemia. Leuk Lymphoma 2019;60:3138-45.

26. Kim B, Lee H, Jang J, Kim SJ, Lee ST, Cheong JW, et al. Targeted next generation sequencing can serve as an alternative to conventional tests in myeloid neoplasms. PLoS One 2019;14:e0212228.

27. Plagnol V, Curtis J, Epstein M, Mok KY, Stebbings E, Grigoriadou S, et al. A robust model for read count data in exome sequencing experiments and implications for copy number variant calling. Bioinformatics 2012;28:2747-54.

28. Kim H, Shim Y, Lee TG, Won D, Choi JR, Shin S, et al. Copy-number analysis by base-level normalization: An intuitive visualization tool for evaluating copy number variations. Clin Genet 2023;103:35-44.

29. Kuilman T, Velds A, Kemper K, Ranzani M, Bombardelli L, Hoogstraat M, et al. CopywriteR: DNA copy number detection from off-target sequence data. Genome Biol 2015;16:49.

30. Nilius-Eliliwi V, Gerding WM, Schroers R, Nguyen HP, Vangala DB. Optical genome mapping for cytogenetic diagnostics in AML. Cancers (Basel) 2023;15.

31. Wang Y, Li J, Xue TL, Tian S, Yue ZX, Liu SG, et al. Clinical, biological, and outcome features of P2RY8-CRLF2 and CRLF2 over-expression in pediatric B-cell precursor acute lymphoblastic leukemia according to the CCLG-ALL 2008 and 2018 protocol. Eur J Haematol 2023;110:669-79.

32. Palmi C, Vendramini E, Silvestri D, Longinotti G, Frison D, Cario G, et al. Poor prognosis for P2RY8-CRLF2 fusion but not for CRLF2 over-expression in children with intermediate risk B-cell precursor acute lymphoblastic leukemia. Leukemia 2012;26:2245-53.

33. Cario G, Zimmermann M, Romey R, Gesk S, Vater I, Harbott J, et al. Presence of the P2RY8-CRLF2 rearrangement is associated with a poor prognosis in non-high-risk precursor B-cell acute lymphoblastic leukemia in children treated according to the ALL-BFM 2000 protocol. Blood 2010;115:5393-7.

34. Ahmadi SE, Rahimi S, Zarandi B, Chegeni R, Safa M. MYC: a multipurpose oncogene with prognostic and therapeutic implications in blood malignancies. J Hematol Oncol 2021;14:121.

35. Hirabayashi S, Ohki K, Nakabayashi K, Ichikawa H, Momozawa Y, Okamura K, et al. ZNF384-related fusion genes define a subgroup of childhood B-cell precursor acute lymphoblastic leukemia with a characteristic immunotype. Haematologica 2017;102:118-29.

36. Skucha A, Ebner J, Grebien F. Roles of SETD2 in leukemia-transcription, DNA-damage, and beyond. Int J Mol Sci 2019;20.

37. Vairy S, Tran TH. IKZF1 alterations in acute lymphoblastic leukemia: the good, the bad and the ugly. Blood Rev 2020;44:100677.